Photosensitive Polyamines for High-Performance Photocontrol of DNA Higher-Order Structure

Anna Venancio-Marques,[†,‡,§] Anna Bergen,[†,‡,§] Caroline Rossi-Gendron,[†,‡,§] Sergii Rudiuk,[†,‡,§] and Damien Baigl[†,‡,§,*]

[†]Ecole Normale Supérieure—PSL Research University, Department of Chemistry, 24 Rue Lhomond, F-75005, Paris, France, [‡]Sorbonne Universités, UPMC Univ Paris 06, PASTEUR, F-75005, Paris, France, and [§]CNRS, UMR 8640 PASTEUR, F-75005, Paris, France

ABSTRACT Polyamines are small, ubiquitous, positively charged molecules that play an essential role in numerous biological processes such as DNA packaging, gene regulation, neuron activity, and cell proliferation. Here, we synthesize the first series of photosensitive polyamines (PPAs) and demonstrate their ability to photoreversibly control nanoscale DNA higher-order structure with high efficiency. We show with fluorescence microscopy imaging that the efficiency of the PPAs as DNA-compacting agents is directly correlated to their molecular charge. Micromolar concentration of the most efficient molecule described here, a PPA containing three charges at neutral pH, compacts DNA molecules from a few kilobase pairs to a few hundred kilobase pairs, while subsequent 3 min UV illuminations at 365 nm triggers complete unfolding of DNA molecules. Additional application of blue light (440 nm for 3 min) induces the refolding of DNA into the compact state. Atomic force microscopy reveals that the compaction involves a global folding of the whole DNA molecule, whereas UV-induced unfolding is a modification initiated from the periphery of the compacted DNA, resulting in the occurrence of intermediate flower-like structures prior to the fully unfolded state.

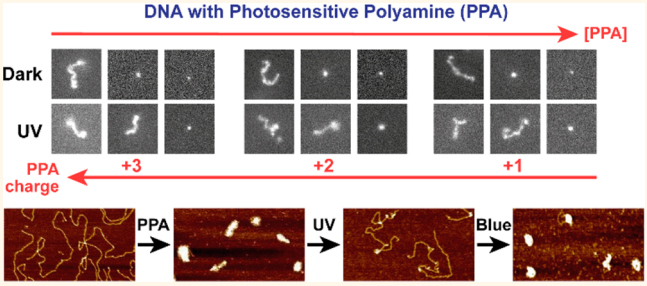

KEYWORDS: polyamines · DNA compaction · photocontrol · DNA · AFM · light

DNA can undergo a dramatic conformational transition from a wormlike coil to a much smaller globular state.[1−3] This phenomenon, known as DNA compaction, is a key biological process involved in the packaging[4] of genetic information as well as in gene regulation.[5−7] The biomedical applications of compaction, such as transfection in gene therapy,[8,9] have triggered strong interest, as have recent developments in bio- and nanotechnologies.[10−12] Compaction of DNA is usually achieved by the addition of compacting agents, which include multivalent organic or inorganic cations, proteins, cationic lipids, and many other positively charged nano-objects.[3,13,14] Naturally occurring polyamines, such as spermidine (3+) or spermine (4+), are omnipresent cellular compounds that can induce DNA compaction thanks to multiple protonated amine groups. They play an essential role in numerous biological processes, as they are involved not only in DNA packaging but also in cellular proliferation and neuron signaling.[15−18] As a result, natural or synthetic polyamines are frequently used as compacting agents for fundamental studies on DNA compaction as well as for transfection applications.[8,19−22] However, once DNA is compacted with polyamines, its decompaction requires changing the chemical composition of the sample, through either dilution of the solution, modification of the pH, or addition of a decompacting agent, usually a lower valence salt.[3,23,24] To achieve compaction or decompaction prompted by an external stimulus, a different strategy needs to be set up. Although temperature-induced DNA compaction strategies have been successfully implemented, significant achievements were usually obtained for temperatures far from a physiologically relevant range.[25] Light is another noninvasive external stimulus especially well-suited for dynamic monitoring of biological systems, due to its high spatial

* Address correspondence to damien.baigl@ens.fr.

Received for review January 15, 2014 and accepted February 28, 2014.

Published online March 01, 2014
10.1021/nn500266b

and temporal resolutions as well as satisfactory biocompatibility.[26] In the past few years, researchers have attempted to trigger DNA compaction and decompaction with adequate illumination conditions by developing photoresponsive compacting agents with potential applications for the photocontrol of transfection,[27] gene expression,[28,29] and enzymatic activity.[30] For most of these molecules, the photosensitivity was due to an azobenzene moiety, able to undergo an isomerization upon appropriate illumination, and the compaction ability was brought about by a single cationic charge or, in a very few cases, two charges.[31−38] The molecules showed different binding affinities to DNA depending on illumination conditions, but light-induced DNA decompaction proved to be challenging. In fact, a light-gated, dynamic compaction/decompaction sequence was achieved in only a few cases, where high amounts of compacting agents and long illumination times were required.[31,35,38] To achieve efficient and photoreversible DNA compaction at much lower compacting agent concentration and reduced illumination time, we explored the use of polyamines, molecules known for their unique ability to reversibly compact DNA, that we made photosensitive through the incorporation of a photoisomerizable azobenzene motif. In this article, we describe the first series of photosensitive polyamines, demonstrating photoreversible and highly efficient compaction of giant and gene-sized DNA molecules, at concentrations 10- to 100-fold lower than usual photoresponsive compacting agents and much reduced illumination time. The effect of molecular charge and the impact of the illumination conditions on DNA compaction and unfolding processes are studied by fluorescence microscopy and atomic force microscopy.

RESULTS AND DISCUSSION

Photosensitive Polyamines. We synthesized three photosensitive polyamines (PPAs), combining an azobenzene unit with side chains containing an increasing number of amine groups (Figure 1). A short $-OCH_2CH_2-$ chain was used as a linker. To obtain a molecule with two amine groups, we attached ethylenediamine (En) to the azobenzene unit and thus synthesized the shortest PPA studied here, **AzoEn**. Using diethylenetriamine (Deta) increased the number of amine groups to three, giving rise to an intermediate molecule, **AzoDeta**. Finally tris(2-aminoethyl)amine (Tren) allowed the synthesis of a final PPA with four amine groups, **AzoTren**.

Information on the synthesis and standard characterizations of these compounds is given in the Experimental Section. The amine pK_a values (SI, Figure S1) were determined by structure-based calculations with MarvinSketch software. From these values, we derived the first important feature of the three molecules, *i.e.*, their charge. In particular, the pH dependency of the

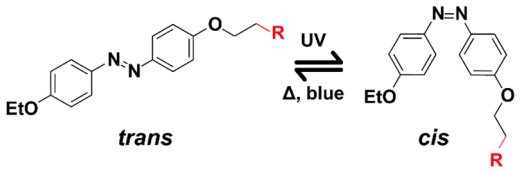

R =	Name
NH_2. HCl	AzoEn
NH_2 . 2 HCl	AzoDeta
NH_2 . 3 HCl	AzoTren

Figure 1. Structures of photosensitive polyamines. The azobenzene moiety found in all compounds undergoes a *trans*−*cis* isomerization under UV illumination (365 nm) and thermally relaxes back in the dark or upon blue light illumination (440 nm). The headgroup is an ethylenediamine entity for AzoEn, a diethylenetriamine for AzoDeta, and tris(2-aminoethyl)amine for AzoTren.

charge was calculated for each molecule with the equations given in the SI, Text S1. Figure 2a shows the evolution of the charge as a function of biologically relevant pH values for the three PPAs. All experiments were performed in a buffer at pH = 7.4, fixing the charge of **AzoEn** to 1.2, of **AzoDeta** to 1.9, and of **AzoTren** to 3.0. By changing the number of amine groups in each of the synthesized molecules, we were therefore able to obtain various positively charged polyamines, with overall charges from 1.2 to 3.0. A second important feature of the polyamines studied here was their photosensitive nature, achieved through the incorporation of an azobenzene motif, for which isomerization from a less polar *trans* state to a more polar *cis* state can be triggered by illumination at the right wavelength.[39] Here, the switch from a *trans*-rich state to a photostationary state where the *cis* isomer is predominant was achieved by UV light (365 nm). We determined the composition of the photostationary states of the three PPAs for dark conditions and for UV illumination by ^{1}H NMR spectroscopy (SI, Figure S2). For PPAs under dark conditions, we found a *trans*/*cis* ratio of about 80:20, while UV illumination led to a ratio of about 30:70 (the composition for each PPA is given in the SI, Table S1). The distinct UV−vis spectra of the two isomers enabled a spectrophotometric study of the kinetics of the isomerization process, as seen for example in Figure 2b for **AzoTren**. The *trans* isomer of all three polyamines displayed a characteristic peak at λ = 356 nm, while the *cis* isomers were characterized by a two-peak spectrum (320 and 430 nm). *Trans*-rich solutions were irradiated for short, 5 s periods at 365 nm

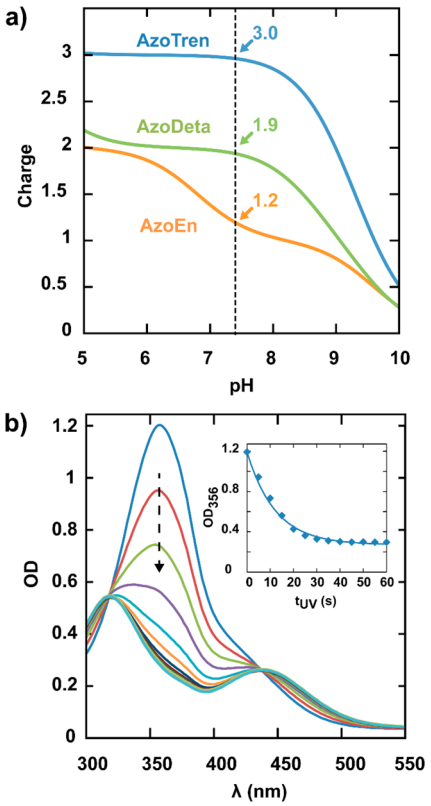

Figure 2. Properties of photosensitive polyamines. (a) Calculated charge as a function of pH, for AzoEn (orange), AzoDeta (green), and AzoTren (blue). Arrows indicate the charge of each molecule for the working pH of 7.4. (b) Absorption spectra of AzoTren (100 μM in water) in the dark (blue) and after various illumination times (t_{UV}). The arrow indicates increasing t_{UV} by increments of 5 s. The inset shows the optical density at 356 nm (OD_{356}) as a function of t_{UV}, where symbols are data points and the solid line is an exponential decay fit with a time constant of 12 s.

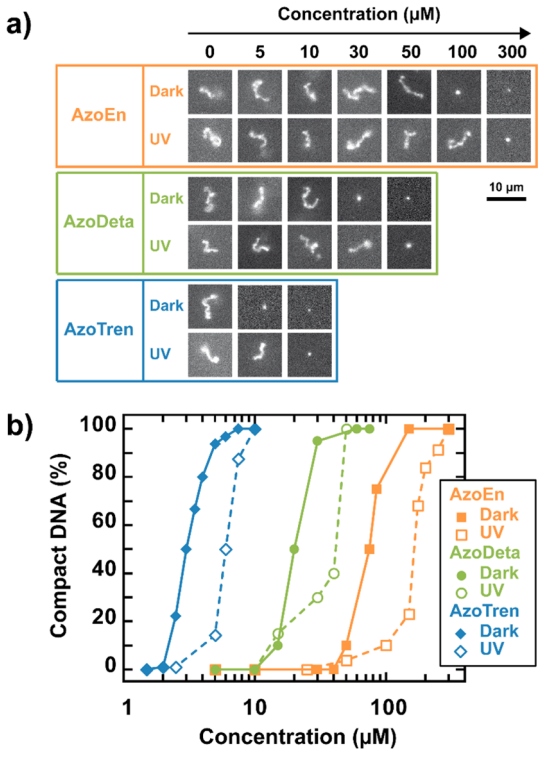

Figure 3. Photosensitive polyamines compact giant genomic DNA in a light-sensitive manner, with marked charge-dependent efficiency. (a) Representative fluorescence microscopy images of individual T4 DNA molecules (166 kbp) stained by YOYO-1 for increasing concentrations of photosensitive polyamines before (dark) and after (UV) illumination at 365 nm. (b) Percentage of DNA molecules in the compact state as a function of polyamine concentration for the three photosensitive polyamines, before (filled symbols) and after (open symbols) UV illumination. Symbols are data points and solid (respectively dashed) lines are guidelines for the eyes for dark (respectively UV) conditions. Conditions: [T4 DNA] = 0.1 μM in 10 mM Tris-HCl (pH = 7.4); YOYO-1 = 0.01 μM; no light (dark) or illumination at 365 nm (UV) for 10 min prior to DNA introduction.

to give the *cis*-rich solutions, leading to similar results for all three polyamines (SI, Figures S3 and S4). For each molecule, the decrease of the optical density at 356 nm was plotted as a function of time, and the resulting curve was fitted with an exponential decay to determine the characteristic time constants (inset Figure 2b and SI, Figures S3−S5).

The isomerization process from the *trans*-rich state to the *cis*-rich state was similar for all three PPAs, as the three time constants were of the same order of magnitude of 10 s (12 s for **AzoEn**, 10 s for **AzoDeta**, and 12 s for **AzoTren**, SI Table S2). The thermal relaxation in the dark of the *cis* isomer to its *trans* counterpart was found to have much longer time scales, typically of a hundred minutes (SI, Table S2 and Figures S6−S8), showing that all *cis* isomers displayed significant thermal stability. As a result, we have synthesized three PPAs with two main characteristics: (i) an overall charge from 1.2 to 3 at pH = 7.4 depending on the number of protonated amine groups and (ii) a phototunable polarity through azobenzene *trans*−*cis* isomerization.

Compaction of Genomic DNA by Photosensitive Polyamines. The compaction efficiency of the synthesized PPAs was determined with long, double-stranded T4 DNA molecules (166 kbp) using fluorescence microscopy imaging. Figure 3a shows representative images of individual DNA molecules in the presence of PPAs at different concentrations under different illumination conditions. In these experiments, a given PPA was kept in the dark or illuminated at 365 nm for 10 min, prior to introduction of YOYO-stained T4 DNA molecules. Two main types of DNA conformations were observed in solution. In the absence of PPA (Figure 3a, first column), DNA molecules appeared as long fluctuating chains and were referred to as unfolded DNA. The elongated coil conformation of DNA was attributed to the electrostatic repulsion between phosphate groups along the backbone of dsDNA. Note that the elongated conformation of individual DNA molecules was also observed for low polyamine concentrations. However, as the polyamine concentrations increased, we observed a transition to a compact state where the majority of DNA molecules appeared as extremely mobile spots with a marked

reduction of size. At even higher concentrations of polyamine, DNA molecules could no longer be observed in solution, most likely due to a displacement of the YOYO-1 dye by the compaction process.[40]

The transition from the unfolded to the compact state was observed for all polyamines but was strongly dependent on both polyamine charge and illumination conditions (Figure 3a). On one hand, comparing the same polyamine solution under different illumination conditions shows that the concentration required to achieve the compaction of DNA molecules was consistently lower when the *trans* isomer was predominant in solution (dark) than when the solution contained a majority of *cis* isomer (UV). Certain concentration ranges therefore compacted DNA under dark conditions, but not after UV illumination. On the other hand, for a fixed configuration of the azobenzene motif (considering either the dark or the UV series), another trend can also be observed, as the concentration needed to achieve DNA compaction strongly decreased when the number of amine groups in the molecule, *i.e.*, the charge of the molecule, increased. For a quantitative analysis of the compaction of genomic DNA molecules by the three polyamines, we established compaction curves giving the percentage of DNA molecules in a compact state as a function of polyamine concentration by analyzing for each set of conditions the conformation of over 150 individual T4 DNA molecules in solution by fluorescence microscopy (Figure 3b). Compaction curves show that for intermediate concentrations compact and elongated DNA molecules coexisted in solution. For dark conditions, this was, for instance, the case for concentrations ranging from 40 to 100 μM for **AzoEn**, from 10 to 30 μM for **AzoDeta**, and finally from 2 to 5 μM for **AzoTren**. Moreover, considering both conditions (dark, UV) for a given polyamine, the curves obtained after UV illumination were always shifted to higher concentrations compared to the curves recorded for dark conditions. Table 1 specifies the polyamine concentration required to compact 50% of the DNA molecules (C_{50}), showing a 2-fold increase in the concentration of the *cis*-rich solution compared to that needed with the *trans*-rich counterpart. The compaction efficiency of the *trans* isomer was therefore systematically higher than that of the *cis* isomer, in agreement with a higher affinity of the less polar *trans* isomer for DNA molecules. A similar trend was described in the case of monocationic photosensitive surfactants[35] but has never been reported for polyamine-based molecules and can be explained as follows. The compaction of DNA by amphiphilic cationic molecules is known to be highly cooperative.[41] As a consequence, for a given polyamine, the less polar *trans* isomer, which is more prone to assembly, is more efficient in cooperatively binding to DNA and inducing DNA compaction than the more polar *cis* isomer.

TABLE 1. Polyamine Concentration (C_{50}) and Charge Ratio (Z^*_{50}) Required to Achieve the Compaction of 50% of DNA Molecules Present in Solution, under Experimental Conditions of Figure 3

	C_{50} (μM)		Z^*_{50}	
	dark	UV	dark	UV
AzoEn (1.2+)	75	160	900	1920
AzoDeta (1.9+)	20	40	380	760
AzoTren (3.0+)	3	6	90	180

Interestingly, the compaction properties were not solely dependent on the isomerization state of the polyamines. Comparing the polyamines for set illumination conditions, we see that their compaction curves were ordered according to the polyamine charge, with **AzoTren** under dark conditions as the most efficient compacting agent, reaching full compaction at 5 μM.

C_{50} values were useful to compare and contrast the compaction efficiencies of the three PPAs according to their charge (Table 1). While increasing the charge from 1.2 to 1.9 from **AzoEn** to **AzoDeta** decreased the concentration required to achieve 50% compaction by a factor of 3.8, increasing the charge to 3 when switching from **AzoDeta** to **AzoTren** led to a further decrease of the C_{50} by a factor of 6.7. The C_{50} ratio of 6.7 between **AzoDeta** (1.9+) and **AzoTren** (3+) was of the same order of magnitude as values reported for nonphotosensitive polyamines, in particular for 1,3-diaminopropane (2+) and spermidine (3+),[22] displaying a concentration ratio for the onset of compaction of about 5. Note that in all cases, for both standard and photosensitive polyamines, the concentrations needed to induce 50% compaction of DNA molecules were higher than the concentration of DNA (0.1 μM in phosphate groups), corresponding to an accumulation of an excess of positive charges in solution before DNA compaction could occur. We therefore computed the charge ratio at 50% of DNA compaction (Z^*_{50}) defined by

$$Z^*_{50} = \frac{ZC_{50}}{[\mathrm{DNA}]}$$

where Z stands for the charge of the polyamine, C_{50} its concentration to achieve 50% of compaction, and [DNA] the concentration of DNA in phosphate groups. Hence, Z^*_{50} represents the ratio of charges provided by the polyamine (ZC_{50}) and the DNA, which has a single negative charge per phosphate group. Therefore, for a given DNA concentration, high Z^*_{50} values mean high charge concentrations are necessary to achieve compaction. When comparing the charge ratio required to compact 50% of the DNA molecules, we noticed that Z^*_{50} decreased by a factor about 2.5 from **AzoEn** to **AzoDeta** and by a factor of 4 from **AzoDeta** to **AzoTren** (Table 1). As a result, the excess of positive charges necessary to trigger DNA compaction in the case of

AzoTren is 10 times lower than the excess observed for **AzoEn**. This shows that the increase in efficiency with the number of positive charges is not solely the result of charge concentration, as the required excess charge should then be the same for all compacting agents, but also of inherent polyamine properties due to the presence of several positive charges within the same molecule. This effect is well known for nonphotosensitive polyamines[21,42] and can be rationalized for our photosensitive polyamines by taking into account the crucial role of DNA counterions (SI, Text S2). As the charge of the polyamine increases, the neutralization of DNA is also enhanced, giving insight into why **AzoTren** is a better compacting agent than **AzoDeta** and **AzoEn**. Furthermore, by establishing the compaction curve for spermine, a well-known, very efficient compacting agent, under the identical experimental conditions as those used for the three PPAs, we were able to compare and contrast PPAs to natural polyamines (SI, Figure S9). In particular we found that the compaction profile obtained for spermine was similar to that obtained for **AzoTren**, as they have the same C_{50} values (3 μM), thus establishing the high efficiency of **AzoTren** as a compacting agent. By analyzing the effect of the buffer on the compaction efficiency of **AzoTren**, we found that the compaction curves for **AzoTren** were shifted to higher concentrations as the buffer concentration increased, with C_{50} values of 3, 8, and 13 μM for Tris-HCl concentrations of 10, 50, and 100 mM, respectively (SI, Figure S10). This is an agreement with trends reported for natural polyamines; that is, higher buffer concentrations mean an increase in monovalent salts in solution that competitively exchange with polyamines, therefore reducing their efficiency in compacting DNA. Despite the many similarities between spermine and **AzoTren**, two marked differences can be emphasized. First and foremost, **AzoTren**, with only three positive charges, has the same compaction efficiency as spermine, a compacting agent with four charges at neutral pH. This underlines the role of the hydrophobic azobenzene tail of **AzoTren**, which promotes DNA compaction by enhancing its cooperative binding to DNA.[35] Second, the compaction of DNA by PPAs can be actuated by light, which is not the case for spermine-mediated compaction (SI, Figure S9), indicating that the effect of light on PPA compaction efficiency is directly due to the polarity change upon azobenzene photoisomerization. All in all, we have shown that the newly described PPAs were able to compact genomic DNA with efficiencies that can be modulated by both their charge and external illumination conditions.

Light-Induced Decompaction and Recompaction of a Linearized Plasmid Compacted by AzoTren. At micromolar concentrations, **AzoTren** proved to be an efficient compacting agent of genomic DNA. To test the interaction between this PPA and much shorter, gene-sized DNA molecules, we explored the compaction of a 4.5 kbp linearized plasmid by **AzoTren**. Since fluorescence microscopy was not suitable for the observation of such small DNA molecules, the study was carried out using atomic force microscopy (AFM) (Figure 4 and SI, Figures S11−S12). We first studied the impact of a

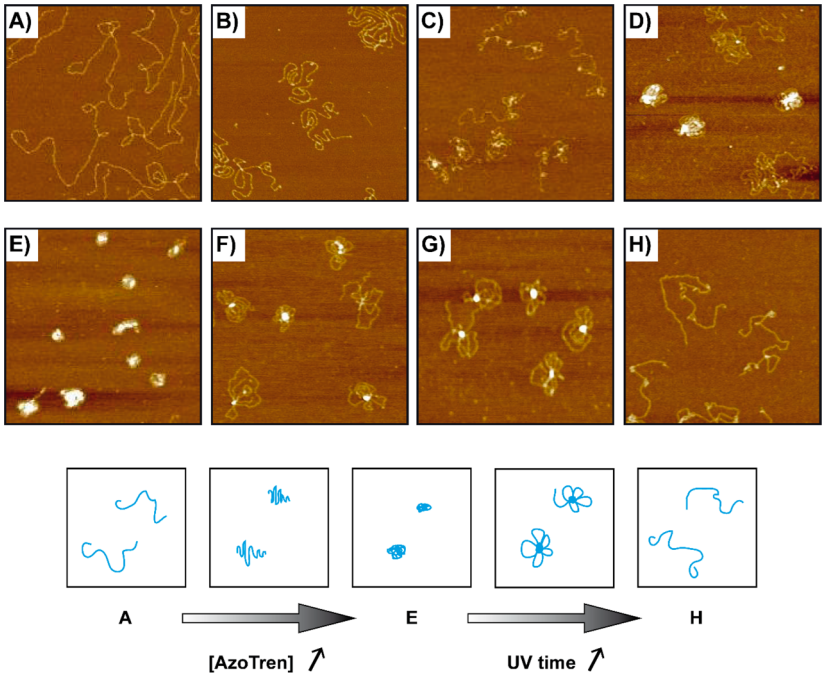

Figure 4. AFM shows the compaction process of a gene-sized linear DNA (4.5 kbp) by AzoTren and its subsequent unfolding by UV. For images A to E the concentration of polyamine increased (respectively 0, 0.5, 2, 4, and 5 μM). For images E to H, DNA was first compacted by AzoTren (5 μM) prior to an increasing exposure to UV at 365 nm (respectively 0, 30, 60, and 180 s). Conditions: [DNA] = 2 μM in 10 mM Tris-HCl (pH = 7.4). All AFM image sizes are 1000 × 1000 nm^2.

gradual increase in the concentration of **AzoTren** (Figure 4A–E). In the absence of compacting agent, the linearized plasmids appear as long, rather stretched out coils with large end-to-end distances (Figure 4A). The vertical scale indicated typical heights of 0.30 ± 0.04 nm, in agreement with previous measurements of double-stranded DNA adsorbed on mica.[43,44] We measured a contour length of 1440 ± 44 nm, a value close to the length of a fully stretched 4.5 kbp DNA (1530 nm). Upon addition of 0.5 μM **AzoTren** (Figure 4B), the appearance of DNA molecules changed significantly. The previously long coils started to bend and twist, resulting in shorter end-to-end distances. As the **AzoTren** concentration was further increased to 2 μM (Figure 4C), the morphology of the DNA objects observed by AFM continued to change, with the appearance of dense spots inside each structure. This evolution was even clearer for [**AzoTren**] = 4 μM, as more than half of the DNA molecules were folded, forming compact DNA objects of an average height of 3.5 ± 0.7 nm (Figure 4D). Finally, for [**AzoTren**] = 5 μM, all DNA molecules were observed as compact objects of an average height of 4.3 ± 1.3 nm, occupying only a fraction of the surface they covered in the absence of compacting agent (Figure 4E).

This morphology was attributed to a fully compact state of DNA. From the various lateral sizes of these compact objects, we inferred that unimolecular compact states probably coexisted with multimolecular aggregates. The behavior of the linearized plasmids undergoing compaction in the presence of **AzoTren** was therefore determined to be similar to that observed by fluorescence microscopy for genomic DNA molecules. We then investigated the effect of UV light on compact DNA (Figure 4E–H). Note that, in this case, light was applied directly on the solution containing DNA already compacted by **AzoTren**. This was achieved by shining UV light (365 nm) for a fixed time (30, 60, and 180 s) on a sample containing fully compacted DNA molecules by 5 μM **AzoTren** and then imaging the sample (Figure 4F–H). A marked unfolding was observed when the sample was illuminated by UV. Notably, the unfolding steps were distinct from the previously studied compaction process. Indeed, under UV illumination, the unfolding of the short DNA molecules occurred from the periphery, around a small compact core, of the same average height as the compacted DNA observed in Figure 4E, resulting in flower-like structures of the DNA molecules (Figure 4F, G). Full decompaction, with elongated molecules of 0.29 ± 0.05 nm in height, was achieved after only 3 min illumination by UV. To have a quantitative description of the compaction/unfolding process, we systematically measured the long-axis length of DNA molecules, defined as the longest distance measured on an adsorbed DNA molecule, and plotted the size distribution (Figure 5). A wide distribution centered on

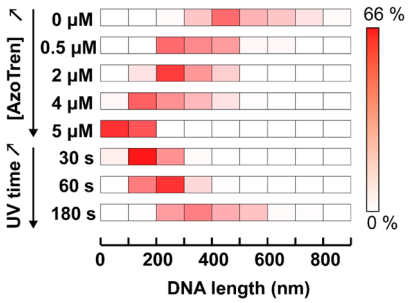

Figure 5. Photoreversibility of AzoTren-based DNA compaction. Distribution of the long-axis length of DNA measured by AFM for an increasing AzoTren concentration (0–5 μM) in the dark and for an increasing UV illumination time at 365 nm (30–180 s) applied on DNA compacted by 5 μM AzoTren. The red color intensity indicates the percentage for each size class. [DNA] = 2 μM in 10 mM Tris-HCl (pH = 7.4).

520 ± 141 nm was obtained in the absence of compacting agent. As the **AzoTren** concentration increased, the long-axis length distributions became much sharper and centered on decreasing values. Full compaction corresponded to an average length of 93 ± 29 nm. Increasing the UV illumination time resulted in the opposite trend, with a sharp distribution getting progressively wider and an increasing average long-axis length. The unfolding of the DNA molecule under UV illumination can be rationalized by considering the isomerization of the *trans*-**AzoTren** to the *cis* isomer induced by UV light (365 nm) described in Figure 2b. As **AzoTren** molecules isomerize due to UV illumination, the concentration of *trans* compacting agent decreases and that of the *cis* isomer increases. Because of the lower affinity of *cis*-**AzoTren** for DNA compared to its *trans* counterpart (Figure 3), the DNA molecules undergo an unfolding process. Note that the UV illumination time required to unfold DNA was significantly longer than that needed to achieve *trans* to *cis* isomerization of **AzoTren** in the absence of DNA. This phenomenon, reported for all photosensitive azobenzene-based compacting agents, is most likely due to the stabilization of the DNA–**AzoTren** complex by hydrophobic interactions through the azobenzene moiety. According to the literature, for markedly more hydrophobic molecules but with a similar compaction efficiency, the stabilization of DNA–compacting agent complexes was so strong that it led to a loss of reversibility and decompaction could not be achieved even for long UV illumination.[35] Here, despite the strong compaction efficiency of **AzoTren**, the decompaction was achieved with comparatively short illumination times. Furthermore, it was possible to recompact the previously UV-decompacted DNA molecules by shining blue light (λ = 440 nm) for 3 min on the sample (SI, Figure S12). These DNA molecules characterized by AFM imaging had a mean size of 115 ± 33 nm, a size comparable to compact DNA molecules before UV illumination. We linked this compaction process to the *cis*-to-*trans* isomerization triggered by blue light,

whereby the concentration of *trans*-**AzoTren** in solution increased again.

The AFM study of the DNA compaction by **AzoTren** established the high-performance compaction efficiency at micromolar range of this photosensitive polyamine, while demonstrating the reversible character of the phenomenon by following the UV-mediated unfolding of DNA molecules and blue-light-triggered DNA recompaction.

CONCLUSION

The series of photosensitive polyamines described in this paper follow the general trends expected from polyamines. They have high compaction efficiencies that increase with the overall charge of the molecule, displaying a charge effect that was stronger than a simple neutralization effect. The azobenzene unit of the molecules not only allows the shortest polyamine, **AzoEn**, to act as a compacting agent despite its small positive charge (1.2+) but also gives all three polyamines photosensitive properties. The *trans*−*cis* isomerization can be seen as a UV-triggered switch for interactions with DNA, due to the higher binding affinity of the *trans* isomer compared to the *cis* isomer, leading to a photoreversibility of the compaction−decompaction process. Although the wide range of experimental conditions makes rigorous comparison with other similar azobenzene-based compacting agents difficult, it is nonetheless possible to establish some major trends in order to compare and contrast the performance of the PPAs seen in this paper with other published photosensitive compacting agents. In general, in the case of compacting agents with a strong affinity for DNA,[34,35,38] photoreversibility could not be achieved. In fact, for most of these molecules, high DNA affinity was obtained by increasing the hydrophobicity of the compacting agents. It is possible that, in such cases, too strong hydrophobic interactions stabilize the compact state, therefore preventing DNA unfolding by light. In contrast, we exploited here an increase in electrostatic interactions provided by high-valence polyamines, resulting in both high affinity and a photoreversible behavior. In the past, photoreversible compaction was mainly obtained with AzoTAB, an azobenzene-containing monovalent cationic compound (SI, Figure S13) able to induce DNA compaction in near-millimolar range.[28,31−33,35] Here, **AzoTren** can induce compaction in the micromolar range, at concentrations about 100-fold smaller than AzoTAB under identical experimental conditions (SI, Figure S14). Furthermore, the 3 min illumination time required for a full decompaction was short, as previously reported time scales were typically about 20 min long. The synthesized PPA with three positive charges can therefore be described as a high-performance, light-responsive DNA-compacting agent. Since DNA compaction/unfolding is a decisive step in fundamental biological processes (*e.g.*, DNA packaging and gene regulation) as well as in transfection applications, the developed PPAs constitute a class of promising agents to bring these operations under the control of a light trigger. In this article, we focused on synthetic polyamine moieties, but our strategy is also readily applicable to natural polyamines such as spermidine (3+) or spermine (4+). Moreover, as the importance of polyamines in biological processes and diseases is not restricted to DNA packaging and transcription/translation regulation, the range of applications for PPAs can most likely be widened far beyond the demonstrated scope of DNA compaction. For instance, due to the critical role of polyamines in the regulation of ion-channels,[15,18,45] their photosensitive counterparts could be used for the photoregulation of neuron activity.[46,47] For their part in cell proliferation, polyamines are now studied in cancer development and therapy,[17] giving their photosensitive derivatives a promising future in novel phototherapeutic strategies.

EXPERIMENTAL SECTION

Materials. Bacteriophage T4 DNA was purchased from Wako Chemicals and YOYO-1 iodide from Life Technologies. The 4.5 kbp linear DNA was obtained by *Nde I* linearization of the Cx43-EGFP gene in the pMA-QA vector.[48] Milli-Q water (Millipore) was used for all experiments. All other chemicals were purchased from Sigma. Mica (potassium aluminosilicate, Muscovite Mica) for atomic force microscopy was from Goodfellow.

NMR Spectroscopy. NMR spectra were recorded on Bruker 250 and 300 MHz spectrometers. The residual solvent protons (^{1}H) or the solvent carbons (^{13}C) were used as internal standards. Data are presented as follows: chemical shift in ppm (δ) (integration, multiplicity, coupling constant). The following abbreviations are used in reporting NMR data: s, singlet; d, doublet; t, triplet; q, quartet; m, multiplet.

Mass Spectroscopy. Mass spectra were recorded by the Ecole Nationale Superieure de Chimie de Paris Mass Spectrometry Services Laboratory using electron impact (EI).

Elemental Analysis. Elemental analyses were performed by the Microanalysis Service of ICSN CNRS.

Organic Synthesis. The PPAs were synthesized by adapting the method described by Hayashita *et al.*[49] and Diguet *et al.*,[35] as shown in the SI, Figure S15.

AzoOH. To a solution of *p*-ethoxyaniline (80.0 mmol, 1 equiv) and sodium nitrite (80.0 mmol, 1 equiv) in a mixture of ethanol/water (1:1, total volume 160 mL) were added concentrated HCl (17 mL) and ice (80 g) at 0 °C. A solution containing phenol (80.0 mmol, 1 equiv) and sodium hydroxide (160 mmol, 2 equiv) in cold water (42 mL) was slowly added to the first one, and the reaction mixture was stirred at room temperature for 90 min. The pH of the solution was adjusted to 1 with HCl. After 30 min, the precipitate was filtered, washed with pure water (4 × 10 mL), and dried under vacuum to give 17.5 g of a brown powder (yield: 90%). ^{1}H NMR (250 MHz, $CDCl_3$): δ 7.9 (4H, m, H_{arom}), 7.0 (4H, m, H_{arom}), 4.1 (2H, q, ^3J = 7 Hz, CH_3-CH_2-O-), 1.4 (3H, t, ^3J = 7 Hz, CH_3-CH_2-O-).

AzoBr. A solution of sodium hydroxide (86.4 mmol, 1.2 equiv) in anhydrous ethanol (350 mL) was treated with **AzoOH**

(72.0 mmol, 1 equiv) and stirred for 30 min before it was added dropwise to 1,2-dibromoethane (216 mmol, 3 equiv) in anhydrous ethanol (160 mL). The mixture was stirred under reflux for 8 h, and after filtration, it was left at room temperature for 2 days. The precipitate (brown flakes) was filtered, washed with pure water, and dried under vacuum (yield: 52%). ^{1}H NMR (250 MHz, $CDCl_3$): δ 7.9 (4H, H_{arom}), 7.0 (4H, H_{arom}), 4.4 (2H, d, ^3J = 6 Hz, $-O-CH_2-CH_2-Br$), 4.0 (2H, q, ^3J = 7 Hz, CH_3-CH_2-O-), 3.6 (2H, d, ^3J = 6 Hz, $-O-CH_2-CH_2-Br$), 1.4 (3H, t, ^3J = 7 Hz, CH_3-CH_2-O-).

General Procedure for Photosensitive Polyamines AzoEn, AzoDeta, and AzoTren. A solution of **AzoBr** in THF was added dropwise to a solution containing a large excess of the appropriate amine at 0 °C. The reaction mixture was stirred vigorously at room temperature for 2 days. After evaporation of the excess reagent in vacuo, the residue was purified by column chromatography (SiO_2; eluent: CH_2Cl_2/MeOH/NEt_3, 95:5:3). The solvent of the relevant fractions was removed in vacuo, and the residue was dissolved in CH_2Cl_2, washed with K_2CO_3, and dried with Na_2SO_4. The solvent was removed in vacuo, and a yellow powder was obtained.

General Procedure for Salts of Photosensitive Polyamines AzoEn·2HCl, AzoDeta·3HCl, and AzoTren·4HCl. The adequate photosensitive polyamine was dissolved in ethanol, before addition of concentrated HCl to give a red powder, which was filtered, washed with anhydrous ethanol, and dried in vacuo (quantitative yield).

AzoEn. From **AzoBr** (3.40 mmol, 1 equiv) and an excess of ethylenediamine (34.0 mmol, 10 equiv), 500 mg of yellow powder was obtained (M = 328.42 g mol^{-1}, yield: 45%). ^{1}H NMR (300 MHz, $CDCl_3$): δ 7.8 (4H, m, H_{arom}), 6.9 (4H, m, H_{arom}), 4.1 (2H, t, ^3J = 5 Hz, CH_2-O), 4.0 (2H, q, ^3J = 7 Hz, CH_3-CH_2-O), 3.0 (2H, t, ^3J = 5 Hz, $-OCH_2CH_2N-$), 2.8 (2H, t, ^3J = 6 Hz ; CH_2-N), 2.7 (2H, t, ^3J = 6 Hz; CH_2-N), 1.4 (3H, t, ^3J = 7 Hz, CH_3-CH_2-O). ^{13}C NMR (300 MHz, $CDCl_3$): δ 124 (CH), 114 (CH), 67.8 ($O-CH_2-CH_2-N$), 63.8 (CH_3-CH_2-O), 52.4 ($N-CH_2-CH_2-NH_2$), 48.7 ($O-CH_2-CH_2-N$), 41.8 ($N-CH_2-CH_2-NH_2$), 14.8 (CH_3). MS (EI): calcd for $C_{18}H_{24}N_4O_2$ $[M + H]^+$ 329.20, found 328.97. **AzoEn**·2HCl: Anal. Calcd for **AzoEn**, $(HCl)_{2.5}$, $(H_2O)_{0.1}$: C 51.30, H 6.40, N 13.30, O 7.97. Found: C 51.30, H 6.25, N 13.23, O 8.09.

AzoDeta. From **AzoBr** (3.40 mmol, 1 equiv) and an excess of diethylenetriamine (34.0 mmol, 10 equiv), 700 mg of yellow powder was obtained (M = 371.48 g mol^{-1}, yield: 55%). ^{1}H NMR (300 MHz, $CDCl_3$): δ 7.8 (4H, m, H_{arom}), 6.9 (4H, m, H_{arom}), 4.1 (2H, t, ^3J = 5 Hz, CH_2-O), 4.0 (2H, q, ^3J = 7 Hz, CH_3-CH_2-O), 3.0 (2H, t, ^3J = 5 Hz, $-OCH_2CH_2N-$), 2.8 (6H, m, CH_2-N), 2.6 (2H, t, ^3J = 6 Hz; CH_2-N), 1.4 (3H, t, ^3J = 7 Hz, CH_3-CH_2-O). ^{13}C NMR (300 MHz, $CDCl_3$): δ 161 (O−CH), 147 (N−CH), 124 (CH), 114 (CH), 67.6 ($O-CH_2-CH_2-N$), 63.8 (CH_3-CH_2-O), 52.6 ($N-CH_2-CH_2-NH_2$), 49.4 ($N-CH_2-CH_2-N$), 48.7 ($O-CH_2-CH_2-N$), 41.8 ($N-CH_2-CH_2-NH_2$), 14.8 (CH_3). MS (EI): calcd for $C_{20}H_{29}N_5O_2$ $[M + H]^+$ 372.24, found 372.5. **AzoDeta**·3HCl: ^{1}H NMR (300 MHz, D_2O): δ 7.7 (4H, m, H_{arom}), 7.0 (4H, m, H_{arom}), 4.3 (2H, t, ^3J = 5 Hz, $-CH_2-O-$), 4.1 (2H, q, J = 7 Hz, CH_3-CH_2-O-), 3.4 (2H, t, ^3J = 5 Hz, $-O-CH_2-CH_2-NH_2^+-$), 3.3 (2H, t, ^3J = 5 Hz, $-H_2N^+-CH_2-$) 3.1 (4H, t, ^3J = 5 Hz, $-H_2N^+-CH_2-CH_2-N-$), 3.0 (2H, t, ^3J = 5 Hz, $-N-CH_2-CH_2-NH_3^+$), 1.3 (3H, t, ^3J = 7 Hz, CH_3-CH_2-O-). Anal. Calcd for **AzoDeta**, $(HCl)_3$, $(H_2O)_{1/3}$: C 49.33, H 6.78, N 14.39, O 7.67. Found: C 49.59, H 6.74, N 13.99, O 7.67.

AzoTren. From **AzoBr** (1.70 mmol, 1 equiv) and an excess of tris(2-aminoethyl)amine (17.0 mmol, 10 equiv), 190 mg of yellow powder was obtained (M = 414.55 g mol^{-1}, yield: 27%). ^{1}H NMR (300 MHz, $CDCl_3$): δ 7.8 (4H, m, H_{arom}), 6.9 (4H, m, H_{arom}), 4.1 (2H, t, ^3J = 5 Hz, $-CH_2-O-$), 4.0 (2H, q, ^3J = 7 Hz, CH_3-CH_2-O-), 3.0 (2H, t, ^3J = 5 Hz, $-O-CH_2-CH_2-N-$), 2.8 (6H, t, ^3J = 6 Hz, $-CH_2-NH-$), 2.6 (2H, t, ^3J = 6 Hz, $-HN-CH_2-CH_2-N-$), 2.5 (4H, t, ^3J = 6 Hz, $-N-CH_2-CH_2-NH_2$), 1.4 (3H, t, ^3J = 7 Hz, CH_3-CH_2-O-). ^{13}C NMR (300 MHz, $CDCl_3$): δ 161 (O−CH), 147 (N−CH), 124 (CH), 114 (CH), 67.6 ($-O-CH_2-CH_2-N-$), 63.8 (CH_3-CH_2-O-), 57.4 ($-N-CH_2-CH_2-NH_2$), 54.2($-N-CH_2-CH_2-NH-$), 47.7 ($-N-CH_2-CH_2-NH-$), 47.5 ($-O-CH_2-CH_2-NH-$), 39.6 ($-N-CH_2-CH_2-NH_2$), 14.8 (CH_3-CH_2-O-). MS (EI): calcd for $C_{22}H_{34}N_6O_2$ $[M + H]^+$ 415.28, found 415.7. **AzoTren**·4HCl: ^{1}H NMR (300 MHz, D_2O): δ 7.7 (4H, m, H_{arom}), 7.0 (4H, m, H_{arom}), 4.3 (2H, t, ^3J = 5 Hz, $-CH_2-O-$), 4.1 (2H, q, ^3J = 7 Hz, CH_3-CH_2-O-), 3.4 (2H, t, ^3J = 5 Hz, $-O-CH_2-CH_2-NH_2^+-$), 3.2 (2H, t, ^3J = 5 Hz, $-H_2N^+-CH_2-CH_2-N-$), 3.0 (4H, t, ^3J = 6 Hz, $-N-CH_2-CH_2-NH_3^+$), 2.8 (2H, t, ^3J = 7 Hz, $-H_2N^+-CH_2-CH_2-N-$), 2.7 (4H, t, ^3J = 6 Hz, $-N-CH_2-CH_2-NH_3^+$), 1.3 (3H, t, ^3J = 7 Hz, CH_3-CH_2-O-) ppm. Anal. Calcd for **AzoTren**$(HCl)_{4.4}(H_2O)_{0.8}$: C 44.82, H 6.85, N 14.26, O 7.60. Found: C 45.07, H 7.17, N 13.9, O 7.53.

Quantification of the *trans*-to-*cis* Ratio by NMR Spectroscopy. The *trans*-to-*cis* ratios of solutions containing **AzoEn**, **AzoDeta**, and **AzoTren** under dark and UV conditions were determined experimentally by means of NMR spectroscopy. Therefore the corresponding PPA was dissolved in D_2O (c_{final} = 1.0 mM) and was kept in the dark until a photostationary state was reached. Afterward a ^{1}H NMR spectrum was recorded at a Bruker spectrometer (300 MHz), and the content of *trans* and *cis* isomers in solution was determined by the intensity ratios of the corresponding integrals of the peaks (see Figure S2 for **AzoTren**). To obtain the data for the *cis*-rich state (UV condition), the sample was irradiated with UV light (λ = 365 nm) until the photostationary state was reached. ^{1}H NMR spectra were recorded subsequently, and the ratios were determined after integration of the corresponding signals. Values are given in the SI, Table S1.

Measurement of Isomerization Time Constants. Absorption spectra were recorded on a Synergy HT spectrophotometer from BioTek. For *trans*-to-*cis* isomerization under UV illumination, the sample concentration was adjusted to maximum optical densities of 1.0 to 1.2. The samples (200 μL in microplate wells) were irradiated at 365 nm for 5 s (samples were placed at 1 cm from a hand-held VL-6 UV lamp). UV−vis spectra (from 300 to 550 nm, optical path of 0.6 cm) were measured over a 2 min time period, and the process was started once again. Note that precautions were taken to limit the exposition of the samples to ambient light. From the collected spectra, the evolution of the optical density at 356 nm was plotted as a function of UV-illumination time for all three photosensitive polyamines (Figure 1c and SI, Figures S3−S5). With the online curve-fitting program ZunZun, the curves were fitted with the equation $y = A + B\exp(-t/\tau_1)$ to give the time constants τ_1 summarized in the main text and in the SI, Table S2. For *cis*-to-*trans* isomerization in the dark at 26 °C, the initial concentration of the samples (200 μL in microplate wells) was adjusted to maximum optical densities of 0.9 to 1.3 prior to 6 min UV irradiation to give starting maximum OD values (t = 0 s) of 0.2 to 0.3. UV−vis spectra were recorded from 300 to 550 nm for various times. From the data collected, the optical density at 356 nm was plotted as a function of time for all three polyamines (Figures S6−S8). The online curve-fitting program ZunZun was used to fit the curves with the equation $y - y_0 = A(1 - \exp(-t/\tau_2))$ with y_0 the optical density at time t = 0, to give the time constant summarized in the SI, Table S2.

Fluorescence Microscopy Imaging. Fluorescence microscopy was performed on a Zeiss inverted microscope equipped with a 100× oil-immersed objective and the filter set 44 from Zeiss (Exc: BP 475/40 nm; Em: BP 530/50 nm). Images were acquired with an EMCCD camera (Photonmax 512B, Princeton Scientific) and Metavue image acquisition software (Molecular Devices). Illumination conditions: A stock solution of photosensitive surfactant was prepared in a 1.5 mL Eppendorf tube and kept in the dark or exposed just prior to sample preparation for 15 min to UV light (365 nm) with a 6 W 365 nm UV lamp (hand-held VL-6 model) for UV conditions and then kept in the dark. The concentration of the stock solution was 5 mM for **AzoEn**, 2.5 mM for **AzoDeta**, and 1.0 mM for **AzoTren**. Preparation of samples: Water, Tris-HCl buffer (pH = 7.4, final concentration 10 mM), photosensitive surfactant (UV or dark conditions), and YOYO-1 iodide (final concentration 0.01 μM) were added in this order and thoroughly mixed in a 1.5 mL Eppendorf tube. T4 DNA was then added to give a final concentration of 0.1 μM in phosphate groups. The sample was homogenized by gently turning upside down the tube 5−7 times. Samples were then allowed to equilibrate for 15 min prior to visualization by fluorescence microscopy.

AFM Imaging. AFM measurements were performed using a 5100 atomic force microscope (Agilent Technologies-Molecular Imaging) operated in the dynamic tip deflection mode (acoustic alternating current mode, AAC). All AFM experiments were performed using silicon FORT probes (Applied NanoStructures, Inc.) in the tapping mode with a spring constant of 3 N m^{-1} at 69 kHz. The images were scanned in topography mode. Solutions of 4.5 kbp linear DNA (2.0 μM in phosphate groups) in a 10 mM Tris-HCl buffer (pH = 7.4) without or with **AzoTren** (0.5, 2.0, 4.0, and 5.0 μM) were prepared. When necessary, a 20 μL amount of the sample was placed on a glass slide and illuminated at a distance of 0.8 cm at 365 or 440 nm with a CoolLED pE-2. A freshly cleaved mica surface was first treated with 200 μM spermine solution for 1 h, rinsed with an excess of water, and stored under a drop of water for up to a few hours. Right after removing water with filter paper (Whatman), a 20 μL drop of a diluted sample solution was then placed on the mica slide. After 1 h of incubation in wet atmosphere at room temperature, the mica plate was rinsed with an excess of water, dried with compressed argon, and left under vacuum for 1 h. AFM imaging was then carried out. The color height scale of all AFM images ranges from −1.5 to +1.1 nm.

Conflict of Interest: The authors declare no competing financial interest.

Supporting Information Available: Text S1 and S2, Tables S1 and S2, Figures S1−S15. This material is available free of charge *via* the Internet at http://pubs.acs.org.

Acknowledgment. We thank P. Paoletti for discussion. This work was supported by the European Research Council (ERC) [European Community's Seventh Framework Programme (FP7/2007-2013)/ERC Grant agreement no. 258782] and the Institut Universitaire de France (IUF). A.V.-M. received a fellowship from ENS de Lyon.

REFERENCES AND NOTES

1. Bloomfield, V. A. DNA Condensation. *Curr. Opin. Struct. Biol.* **1996**, *6*, 334–341.
2. Bloomfield, V. A. DNA Condensation by Multivalent Cations. *Biopolymers* **1997**, *44*, 269–282.
3. Estévez-Torres, A.; Baigl, D. DNA Compaction: Fundamentals and Applications. *Soft Matter* **2011**, *7*, 6746–6756.
4. Cerritelli, M. E.; Cheng, N.; Rosenberg, A H.; McPherson, C. E.; Booy, F. P.; Steven, A C. Encapsidated Conformation of Bacteriophage T7 DNA. *Cell* **1997**, *91*, 271–280.
5. Richards, E. J.; Elgin, S. C. R. Epigenetic Codes for Heterochromatin Formation and Silencing: Rounding up the Usual Suspects. *Cell* **2002**, *108*, 489–500.
6. Browning, D. F.; Busby, S. J. The Regulation of Bacterial Transcription Initiation. *Nat. Rev. Microbiol.* **2004**, *2*, 57–65.
7. Dillon, S. C.; Dorman, C. J. Bacterial Nucleoid-Associated Proteins, Nucleoid Structure and Gene Expression. *Nat. Rev. Microbiol.* **2010**, *8*, 185–195.
8. Vijayanathan, V.; Thomas, T.; Thomas, T. J. DNA Nanoparticles and Development of DNA Delivery Vehicles for Gene Therapy. *Biochemistry* **2002**, *41*, 14085–14094.
9. Demeneix, B.; Hassani, Z.; Behr, J.-P. Towards Multifunctional Synthetic Vectors. *Curr. Gene Ther.* **2004**, *4*, 445–455.
10. Zinchenko, A. A.; Yoshikawa, K.; Baigl, D. DNA-Templated Silver Nanorings. *Adv. Mater.* **2005**, *17*, 2820–2823.
11. Rothemund, P. W. K. Folding DNA to Create Nanoscale Shapes and Patterns. *Nature* **2006**, *440*, 297–302.
12. Saccà, B.; Niemeyer, C. M. DNA Origami: The Art of Folding DNA. *Angew. Chem., Int. Ed.* **2012**, *51*, 58–66.
13. He, S.; Arscott, P. G.; Bloomfield, V. A. Condensation of DNA by Multivalent Cations: Experimental Studies of Condensation Kinetics. *Biopolymers* **2000**, *53*, 329–341.
14. Montier, T.; Benvegnu, T.; Jaffrès, P.-A.; Yaouanc, J.-J.; Lehn, P. Progress in Cationic Lipid-Mediated Gene Transfection: A Series of Bio-Inspired Lipids as an Example. *Curr. Gene Ther.* **2008**, *8*, 296–312.
15. Igarashi, K.; Kashiwagi, K. Modulation of Cellular Function by Polyamines. *Int. J. Biochem. Cell Biol.* **2010**, *42*, 39–51.
16. Agostinelli, E.; Marques, M. P. M.; Calheiros, R.; Gil, F. P. S. C.; Tempera, G.; Viceconte, N.; Battaglia, V.; Grancara, S.; Toninello, A. Polyamines: Fundamental Characters in Chemistry and Biology. *Amino Acids* **2010**, *38*, 393–403.
17. Pegg, A. Mammalian Polyamine Metabolism and Function. *IUBMB Life* **2009**, *61*, 880–894.
18. Williams, K. Modulation and Block of Ion Channels: A New Biology of Polyamines. *Cell. Signalling* **1997**, *9*, 1–13.
19. Gosule, L. C.; Schellman, J. A. Compact Form of DNA Induced by Spermidine. *Nature* **1976**, *259*, 333–335.
20. Chattoraj, D. K.; Gosule, L. C.; Schellman, J. A. DNA Condensation with Polyamines. *J. Mol. Biol.* **1978**, *121*, 327–337.
21. Wilson, R. W.; Bloomfield, V. A. Counterion-Induced Condensation of Deoxyribonucleic Acid. A Light-Scattering Study. *Biochemistry* **1979**, *18*, 2192–2196.
22. Takahashi, M.; Yoshikawa, K.; Vasilevskaya, V. V; Khokhlov, A. R. Discrete Coil−Globule Transition of Single Duplex DNAs Induced by Polyamines. *J. Phys. Chem. B* **1997**, *101*, 9396–9401.
23. Cinque, L.; Ghomchi, Y.; Chen, Y.; Bensimon, A.; Baigl, D. Protection of Human Genomic DNA from Mechanical Stress by Reversible Folding Transition. *ChemBioChem* **2010**, *11*, 340–343.
24. Rudiuk, S.; Venancio-Marques, A.; Baigl, D. Enhancement and Modulation of Enzymatic Activity through Higher-Order Structural Changes of Giant DNA-Protein Multibranch Conjugates. *Angew. Chem., Int. Ed.* **2012**, *51*, 12694–12698.
25. Saito, T.; Iwaki, T.; Yoshikawa, K. Why Is the Compact State of DNA Preferred at Higher Temperature? Folding Transition of a Single DNA Chain in the Presence of a Multivalent Cation. *Europhys. Lett.* **2005**, *71*, 304–310.
26. Brieke, C.; Rohrbach, F.; Gottschalk, A.; Mayer, G.; Heckel, A. Light-Controlled Tools. *Angew. Chem., Int. Ed.* **2012**, *51*, 8446–8476.
27. Liu, Y.-C.; Le Ny, A.-L. M.; Schmidt, J.; Talmon, Y.; Chmelka, B. F.; Lee, C. T. Photo-Assisted Gene Delivery Using Light-Responsive Catanionic Vesicles. *Langmuir* **2009**, *25*, 5713–5724.
28. Estévez-Torres, A.; Crozatier, C.; Diguet, A.; Hara, T.; Saito, H.; Yoshikawa, K.; Baigl, D. Sequence-Independent and Reversible Photocontrol of Transcription/Expression Systems Using a Photosensitive Nucleic Acid Binder. *Proc. Natl. Acad. Sci. U.S.A.* **2009**, *106*, 12219–12223.
29. Rudiuk, S.; Saito, H.; Hara, T.; Inoue, T.; Yoshikawa, K.; Baigl, D. Light-Regulated mRNA Condensation by a Photosensitive Surfactant Works as a Series Photoswitch of Translation Activity in the Presence of Small RNAs. *Biomacromolecules* **2011**, *12*, 3945–3951.
30. Venancio-Marques, A.; Liu, Y.-J.; Diguet, A.; di Maio, T.; Gautier, A.; Baigl, D. Modification-Free Photocontrol of β-Lactam Conversion with Spatiotemporal Resolution. *ACS Synth. Biol.* **2012**, *1*, 526–531.
31. Le Ny, A.-L. M.; Lee, C. T. Photoreversible DNA Condensation Using Light-Responsive Surfactants. *J. Am. Chem. Soc.* **2006**, *128*, 6400–6408.
32. Le Ny, A.-L. M.; Lee, C. T. Conformation and Dynamics of DNA Molecules during Photoreversible Condensation. *Biophys. Chem.* **2009**, *142*, 76–83.
33. Sollogoub, M.; Guieu, S.; Geoffroy, M.; Yamada, A.; Estévez-Torres, A.; Yoshikawa, K.; Baigl, D. Photocontrol of Single-Chain DNA Conformation in Cell-Mimicking Microcompartments. *ChemBioChem* **2008**, *9*, 1201–1206.
34. Geoffroy, M.; Faure, D.; Oda, R.; Bassani, D. M.; Baigl, D. Photocontrol of Genomic DNA Conformation by Using a Photosensitive Gemini Surfactant: Binding Affinity *versus* Reversibility. *ChemBioChem* **2008**, *9*, 2382–2385.
35. Diguet, A.; Mani, N. K.; Geoffroy, M.; Sollogoub, M.; Baigl, D. Photosensitive Surfactants with Various Hydrophobic Tail Lengths for the Photocontrol of Genomic DNA Conformation with Improved Efficiency. *Chem.—Eur. J.* **2010**, *16*, 11890–11896.
36. Xing, X.; Wang, X.; Xu, L.; Tai, Y.; Dai, L.; Zheng, X.; Mao, W.; Xu, X.; Zhou, X. Light-Driven Conformational Regulation of Human Telomeric G-Quadruplex DNA in Physiological Conditions. *Org. Biomol. Chem.* **2011**, *9*, 6639–6645.

37. Zakrevskyy, Y.; Kopyshev, A.; Lomadze, N.; Morozova, E.; Lysyakova, L.; Kasyanenko, N.; Santer, S. DNA Compaction by Azobenzene-Containing Surfactant. *Phys. Rev. E* **2011**, *84*, 021909.
38. Zinchenko, A. A.; Tanahashi, M.; Murata, S. Photochemical Modulation of DNA Conformation by Organic Dications. *ChemBioChem* **2012**, *13*, 105–111.
39. Beharry, A. A.; Woolley, G. A. Azobenzene Photoswitches for Biomolecules. *Chem. Soc. Rev.* **2011**, *40*, 4422–4437.
40. Günther, K.; Mertig, M.; Seidel, R. Mechanical and Structural Properties of YOYO-1 Complexed DNA. *Nucleic Acids Res.* **2010**, *38*, 6526–6532.
41. Hayakawa, K.; Santerre, J. P.; Kwak, J. C. T. The Binding of Cationic Surfactants by DNA. *Biophys. Chem.* **1983**, *17*, 175–181.
42. Baigl, D.; Yoshikawa, K. Dielectric Control of Counterion-Induced Single-Chain Folding Transition of DNA. *Biophys. J.* **2005**, *88*, 3486–3493.
43. Hansma, H. G.; Golan, R.; Hsieh, W.; Lollo, C. P.; Mullen-Ley, P.; Kwoh, D. DNA Condensation for Gene Therapy as Monitored by Atomic Force Microscopy. *Nucleic Acids Res.* **1998**, *26*, 2481–2487.
44. Golan, R.; Pietrasanta, L. I.; Hsieh, W.; Hansma, H. G. DNA Toroids: Stages in Condensation. *Biochemistry* **1999**, *38*, 14069–14076.
45. Masuko, T.; Kusama-Eguchi, K.; Sakata, K.; Kusama, T.; Chaki, S.; Okuyama, S.; Williams, K.; Kashiwagi, K.; Igarashi, K. Polyamine Transport, Accumulation, and Release in Brain. *J. Neurochem.* **2003**, *84*, 610–617.
46. Szobota, S.; Gorostiza, P.; Del Bene, F.; Wyart, C.; Fortin, D. L.; Kolstad, K. D.; Tulyathan, O.; Volgraf, M.; Numano, R.; Aaron, H. L.; *et al*. Remote Control of Neuronal Activity with a Light-Gated Glutamate Receptor. *Neuron* **2007**, *54*, 535–345.
47. Gorostiza, P.; Isacoff, E. Y. Optical Switches for Remote and Noninvasive Control of Cell Signaling. *Science* **2008**, *322*, 395–399.
48. Liu, Y.-J.; Hansen, G. P. R.; Venancio-Marques, A.; Baigl, D. Cell-Free Preparation of Functional and Triggerable Giant Proteoliposomes. *ChemBioChem* **2013**, *14*, 2243–2247.
49. Hayashita, T.; Kurosawa, T.; Miyata, T.; Tanaka, K.; Igawa, M. Effect of Structural Variation Within Cationic Azo-Surfactant upon Photoresponsive Function in Aqueous Solution. *Colloid Polym. Sci.* **1994**, *272*, 1611–1619.